MOLECULAR AND CELLULAR BIOLOGY, Mar. 2006, p. 1710–1721 Vol. 26, No. 5
0270-7306/06/$08.00+0 doi:10.1128/MCB.26.5.1710–1721.2006

Requirement of Fission Yeast Cid14 in Polyadenylation of rRNAs

Thein Z. Win,[1] Simon Draper,[2]† Rebecca L. Read,[2] James Pearce,[1] Chris J. Norbury,[3] and Shao-Win Wang[1]*

Department of Zoology, University of Oxford, South Parks Road, Oxford OX1 3PS, United Kingdom[1]; Cancer Research UK Laboratories, University of Oxford, Weatherall Institute of Molecular Medicine, John Radcliffe Hospital, Oxford OX3 9DS, United Kingdom[2]; and Sir William Dunn School of Pathology, University of Oxford, South Parks Road, Oxford OX1 3RE, United Kingdom[3]

Received 25 October 2005/Returned for modification 18 November 2005/Accepted 14 December 2005

Polyadenylation in eukaryotes is conventionally associated with increased nuclear export, translation, and stability of mRNAs. In contrast, recent studies suggest that the Trf4 and Trf5 proteins, members of a widespread family of noncanonical poly(A) polymerases, share an essential function in *Saccharomyces cerevisiae* that involves polyadenylation of nuclear RNAs as part of a pathway of exosome-mediated RNA turnover. Substrates for this pathway include aberrantly modified tRNAs and precursors of snoRNAs and rRNAs. Here we show that Cid14 is a Trf4/5 functional homolog in the distantly related fission yeast *Schizosaccharomyces pombe*. Unlike *trf4 trf5* double mutants, cells lacking Cid14 are viable, though they suffer an increased frequency of chromosome missegregation. The Cid14 protein is constitutively nucleolar and is required for normal nucleolar structure. A minor population of polyadenylated rRNAs was identified. These RNAs accumulated in an exosome mutant, and their presence was largely dependent on Cid14, in line with a role for Cid14 in rRNA degradation. Surprisingly, both fully processed 25S rRNA and rRNA processing intermediates appear to be channeled into this pathway. Our data suggest that additional substrates may include the mRNAs of genes involved in meiotic regulation. Polyadenylation-assisted nuclear RNA turnover is therefore likely to be a common eukaryotic mechanism affecting diverse biological processes.

In eukaryotic cells, most genes are transcribed into precursor messenger RNAs that have to undergo several processing events before maturation, including addition of a cap structure to the 5′ terminus, removal of introns by splicing, and 3′ cleavage and polyadenylation. A key player in the polyadenylation process is the nuclear poly(A) polymerase (PAP), part of a large cleavage and polyadenylation complex that becomes activated during transcription by RNA polymerase II. The poly(A) tail is a hallmark of mRNA and is necessary both for subsequent transport into the cytoplasm and efficient translation. Shortening of the poly(A) tail in the cytoplasm can trigger translational repression and acts as a signal for rapid decay of transcripts (50).

In addition to the canonical nuclear enzyme, eukaryotic cells contain several unconventional PAPs. In a study of the fission yeast *Schizosaccharomyces pombe* we previously identified the *cid1* gene family, which encodes a distinct group of PAPs conserved from yeast to humans (46). In *Caenorhabditis elegans*, the Cid1-related protein GLD-2 was characterized as a cytoplasmic PAP (42), and *Xenopus laevis* GLD-2 was subsequently found to be required for CPEB-mediated cytoplasmic polyadenylation during early development (3). Kwak et al. (20) recently described five human orthologs of the Cid1 protein, named Hs1 to Hs5. Among these, Hs4 is responsible for the synthesis of long poly(A) tails in human mitochondria (37). Sequence comparisons identify six members of the *S. pombe* *cid1* gene family (*cid1*, *cid11*, *cid12*, *cid13*, *cid14*, and *cid16*) (46). Cid1 (for *c*affeine-*i*nduced *d*eath suppressor), the first member of this family to be described, was identified through its ability when overexpressed to confer resistance specifically to the combination of hydroxyurea and caffeine, which overrides the replication checkpoint (44). Cid13 was identified independently based on its ability, when overexpressed, to rescue the hydroxyurea sensitivity of checkpoint *rad* mutants (29, 31). In addition to its related role in checkpoint control, Cid12 is required for faithful chromosome segregation and RNA interference-mediated heterochromatin assembly at centromeres (24, 46). Purified recombinant Cid1 catalyzed polyadenylation in vitro (29), as did Cid13-myc immunoprecipitated from *S. pombe* (31). Both Cid1 and Cid13 are cytoplasmic proteins, indicating that their function is likely to be distinct from that of the nuclear PAP. It has been proposed that Cid13 acts to extend the poly(A) tails of ribonucleotide reductase mRNA to counteract deadenylation and enhance protein synthesis (31).

In *Saccharomyces cerevisiae* the Cid1-related protein Trf4 (which has a redundant homolog, Trf5) was reported to have DNA polymerase activity in vitro (47). Subsequently, immunoprecipitates of Trf4-hemagglutinin (HA) from *S. cerevisiae* were found to have PAP, but not DNA polymerase, activity (31). However, unlike most of the Cid proteins, Trf4 and Trf5 are nuclear (12) and are proposed to function in a nuclear RNA surveillance system, whereby the Trf4-mediated oligoadenylation of RNAs targets them for rapid degradation by the exosome. This resembles the role of polyadenylation in bacterial RNA turnover (15, 21, 40, 51).

In this study, we describe the characterization of fission yeast Cid14, a functional homologue of *S. cerevisiae* Trf4/5. We

* Corresponding author. Mailing address: Department of Zoology, University of Oxford, South Parks Road, Oxford OX1 3PS, United Kingdom. Phone: 44 1865 271212. Fax: 44 1865 271192. E-mail: shaowin.wang@zoo.ox.ac.uk.

† Present address: Wellcome Trust Centre for Human Genetics, University of Oxford, Roosevelt Drive, Oxford OX3 7BN, United Kingdom.

TABLE 1. Yeast strains used in this study

Strain	Genotype	Source or reference
972	*h*$^-$	Lab stock
SW0962	*h*$^-$ *cid14*::*ura4 ura4*	This study
SW0139	*h*$^-$ *cid14*::*LEU2 leu1 ura4*	This study
SW0269	*h*$^-$ *top1*::*LEU2 leu1 ura4*	41
SW0130	*h*$^-$ *cid14*::*ura4 top1*::*LEU2 leu1 ura4*	This study
SW0155	*h*$^-$ *cid14-GFP*::*kan*^{r} *leu1 ura4*	This study
SW0295	*h*$^-$ *nda3-KM311 cid14-GFP*::*kan*^{r} *leu1 ura4*	This study
SW0106	*h*$^-$ *cid14-HA*::*kan*^{r} *leu1 ura4*	This study
SW0161	*h*$^-$ *cdc25-22 cid14-HA*::*kan*^{r}	This study
SW0292	*h*$^-$ *ndc80-GFP*::*kan*^{r} *leu1 ura4*	49
SW0305	*h*$^+$ *nda3-KM311 ndc80-GFP*::*kan*^{r} *leu1 ura4 his2*	45
SW0563	*h*$^+$ *cid14*::*ura4 nda3-KM311 ndc80-GFP*::*kan*^{r} *leu1 ura4 his2*	This study
SW0646	*h*$^-$ *cid12*::*ura4 ura4*	46
SW0554	*h*$^+$ *cid12*::*ura4 nda3-KM311 ndc80-GFP*::*kan*^{r} *leu1 ura4 his2*	This study
SW0240	*h*$^-$ *gar2*-GFP::*kan*^{r} *leu1 ura4*	34
SW0131	*h*$^+$ *cid14*::*ura4 gar2*-GFP::*kan*^{r} *leu1 ura4*	This study
SW0231	*h*$^-$ *bub1*::*LEU2 ade6 leu1 ura4 his1*	4
SW0262	*h*$^-$ *mad2*::*ura4 ade6 leu1 ura4*	10
SW1092	*h*$^-$ *dis3-54*	17
SW1195	*h*$^+$ *dis3-54 cid14*::*ura4 ura4*	This study
SW0428	*h*$^-$ *pat1-114*	Lab stock
CY950[a]	*MAT***a** *trf4ts top1*::*LEU2 ura3 ade2 his3 leu2 trp1*	7

[a] *S. cerevisiae* strain.

present evidence that Cid14 is required for the polyadenylation of rRNAs as a prelude to their degradation by the exosome. Polyadenylation mediated by Cid1-related proteins therefore appears to have different consequences and to affect diverse functions, depending on the subcellular localization and identity of the target RNA.

MATERIALS AND METHODS

Fission yeast strains and methods. Conditions for growth, maintenance, and genetic manipulation of fission yeast were as described previously (23). A complete list of the strains used in this study is given in Table 1. Except where stated otherwise, strains were grown at 30°C in YE5S or EMM2 medium (23) with appropriate supplements. Meiosis and sporulation were induced by plating onto malt extract agar, and tetrad dissection was performed with an MSM micromanipulator (Singer Instruments, Watchet, United Kingdom). Cell concentration was determined with a Sysmex F-800 cell counter (TOA Medical Electronic, Kobe, Japan).

Minichromosome loss rates were measured as described previously (1). Briefly, cells from ade$^+$ colonies were plated on yeast extract (YE) plates and incubated at 30°C for 5 days. The colonies with red sectors covering at least one-half of the colony were counted. The rate of chromosome loss per division is the number of these half-sectored colonies divided by the total number of white colonies plus half-sectored colonies.

Plasmids and site-directed mutagenesis. Plasmid pCB427 (*TRF4 URA3 CEN*) was kindly provided by M. F. Christman (7). Plasmids for overexpression of *cid1* and *cid14* under the control of the *GAL1* promoter were constructed by PCR amplification of the *cid1*$^+$ and *cid14*$^+$ open reading frames from *S. pombe* genomic DNA using the primer pairs CGCGGATCCGCGAATATGAACATTTCTTCT GCAC and ATAGTTTAGCGGCCGCATTCTTATTCACTCAGAATTGTCAC CATC and CGCGGATCCGCGGAGATGGGTAAAAAAAGCGTGTC and AT AGTTTAGCGGCCGCATTCTTATCTAAAAACGTTTGCGTATTTTTTTCGC, respectively, followed by digestion with BamHI and NotI and subsequent ligation into BamHI- and NotI-cleaved pYES2 (Invitrogen), generating pYES2*cid1* and pYES2*cid14*. pREP1*cid14* was constructed by PCR amplification of the *cid14* open reading frame from *S. pombe* genomic DNA using the primer pair CID14F (TTTGGATCCCATGGGTAAAAAAAGCGTGTCATTTAACCGC) and CID14R (TTTGGATCCCTAAAAACGTTTGCGTATTTTTTTCGCTCG), followed by digestion with BamHI and subsequent ligation into BamHI-cleaved pREP1. PCR using primers CID14R and DADAF (CCAAATTATATTTACCTACTTC AGCTCTTGCTCTTGTAATAATATCACCTGAG) and primers CID14F and DADAR (CTCAGGTGATATTATTACAAGAGCAAGAGCTGAAGTAGG TAAATATAATTTGG) was used to generate the *cid14* open reading frame in two fragments overlapping by 53 bp, with the region of overlap spanning codons 298 and 300, which were altered in the primer sequence to encode alanine rather than the aspartate residues specified by the wild-type gene at these positions. The resulting fragments were mixed and used in a secondary PCR with primers CID12F and CID12R. After digestion with BamHI, the final product was ligated into pREP1 to generate pREP1*cid14DADA*. All plasmid constructions were confirmed by complete sequencing of the inserts using an ABI sequencer and ABI PRISM dRhodamine reagents (Applera UK).

Gene disruption. The one-step disruption method was used following PCR-mediated generation of the entire *ura4*$^+$ gene flanked by 80-bp segments from the 5′ and 3′ regions of *cid14*$^+$ using oligonucleotides TGGTTCAATTAGTCA TATATTGATTTTTATAAGAATTCTACAAGATAGGTATAGAAAACCAT TCTATCCATGTCTTAGAGAAATCCCACTGGCTATATGT and ACATT TTAACATATGCTCACGATGTTGACGAACCCCTTCATCAACTGATAAT ATGGTACTTAGGATACTAGGGAAATCTTAATTCTAAATGCCTTCTG AC. Construction of the chromosomally HA- and green fluorescent protein (GFP)-tagged *cid14* strains (*cid14-HA* and *cid14-GFP*) was accomplished by an analogous method using primers CGGAAGACGAAGTACCTATTATTGAGG ACACCACTGCTTCAGATGAAGAATCTCGAGCGAAAAAAATACGCAA ACGTTTTCGGATCCCCGGGTTAATTAA and AAAATTACTACAGATCC ATAGTGAGTTTAAGGTGTTGATTAATTTATTACTGGTATTCGAGTTT ACTGGCTAAATCGTAAGAATTCGAGCTCGTTTAAAC. The *cid14*::*LEU2* allele was generated by a secondary one-step disruption of the *cid14*::*ura4*$^+$ allele using primers as described previously (46).

Antibodies and immunoblotting. Cell extracts were prepared by trichloroacetic acid precipitation following glass bead disruption (6). Immunoblotting was performed essentially as described elsewhere (2). The mouse anti-influenza virus HA monoclonal antibody HA-11 (Babco, Berkeley, CA) was used for detection of HA-tagged Cid14 proteins. Cdc2 was detected using the mouse monoclonal antibody Y100 (generated by J. Gannon and kindly provided by H. Yamano). Horseradish peroxidase-conjugated anti-mouse antibodies (Sigma, Poole, United Kingdom) and enhanced chemiluminescence (ECL; Amersham) were used to detect bound antibody.

Gel filtration chromatography. Chromatographic separation of *S. pombe* lysate from a 100-ml culture of the *cid14-HA* strain in midexponential growth was carried out using a Superose-6 column attached to an fast protein liquid chromatography workstation (Amersham Pharmacia) as previously described (45). The eluate was collected in 0.5-ml fractions, and these were analyzed by sodium dodecyl sulfate-polyacrylamide gel electrophoresis (SDS-PAGE) and immunoblotting. The column was calibrated using the standards dextran blue (~2,000

kDa), thyroglobulin (669 kDa), apoferritin (443 kDa), β-amylase (200 kDa), bovine serum albumin (66 kDa), and carbonic anhydrase (29 kDa).

Microscopy. Visualization of GFP in living cells, embedded in 0.6% low-melting-point agarose after staining with Hoechst 33342 (5 μg/ml), was performed at room temperature as previously described (45). Images were acquired using a Zeiss Axioplan 2 microscope equipped with a Planapochromat 100× objective, an Axiocam cooled charge-coupled device camera, and Axiovision software (Carl Zeiss, Welwyn Garden City, United Kingdom) and were assembled using Adobe PhotoShop.

RNA isolation and quantitative PCR. Total RNA was isolated by hot-phenol extraction and purified using RNeasy (QIAGEN). Total *S. pombe* RNA (0.5 μg) was reverse transcribed (SuperScript; Invitrogen) using an oligo(dT) primer according to the manufacturer's instructions. Quantitative PCR was performed using SYBR green PCR Master Mix (Applera UK) and primer pairs specific for *ste11* (ATACCTGGAGAAGCGACGAA and GAATGAGCGGCGAACTCA TA), *mei2* (TATGGACGAGAACCCTGCTT and GACGTGCATTATTGGG AGCA), and *cdc2* (normalizer gene; CCAGCTAGTGAACGGTGTAA and TC CGCAAAGGGACACCAAAT). Samples were run in triplicate on the Applied Biosystems 7300 real-time PCR system (Applera UK). Relative quantities of transcript were determined using the $2^{-\Delta\Delta Ct}$ formula, where Ct is defined as the cycle at which fluorescence is determined to be statistically above background, ΔCt is the difference in Ct of the gene of interest and Ct of the normalizer gene, and ΔΔCt is the difference in ΔCt of the strain tested and ΔCt of the control cells.

PCR poly(A) test. Polyadenylation tests were performed according to the rapid amplification of cDNA ends-polyadenylation technique (RACE-PAT) method as described previously (32) using a reverse transcription-PCR (RT-PCR) kit (SuperScript; Invitrogen) with oligo(dT) anchor primer AT (GCGAGCTCCGC GGCCGCGT$_{12}$) and a primer specific for 25S rRNA (25F1: GCGGCTGCCT GACAAGGCAATGCCGCGGAG), 5.8S rRNA (5.8F1: TCAGCAACGGATC TCTTGGCTCTCGCATCG), or 5S rRNA (5F1: GTTCCCGTCCGATCACTG CAGTTAAGCGTC). PCR products were cloned (TOPO TA cloning; Invitrogen) and sequenced using an ABI sequencer and ABI PRISM dRhodamine reagents (Applera UK). For detection of mature rRNA, primer pairs 25F2 (GAAGATGGGCGATGGTTGATGAAACGGAAGTG) and 25R1 (ACAAA TCTTGGGAACAAAGGCTTAATCTCAGCAG), 5.8F1 and 5.8R1 (AATGA CACTCAAACAGGCATGCCTTTGGTAG), and 5F1 and 5R1 (AGCCTACA GCACCCCGGATTCCCATGTTGT) were used for 25S, 5.8S, and 5S rRNA, respectively.

RESULTS

***S. pombe cid14*$^+$ is a functional homologue of *S. cerevisiae TRF4*.** Fission yeast contains six *cid1*-like genes, whereas budding yeast has just two, *TRF4* and *TRF5*, which share an essential function as *trf4 trf5* double mutants are inviable. We set out to determine which *cid* gene performs a *TRF4/5*-like function in *S. pombe*. Sequence comparisons identified Cid14 as the closest relative of Trf4/5 (Fig. 1A). We therefore asked whether or not *cid14*$^+$ could rescue the phenotype of *trf4* mutants. In *S. cerevisiae*, *TRF4* and *TRF5* were identified through mutations that are synthetically lethal with a mutation in DNA topoisomerase I (7). To determine if *cid14*$^+$ could complement this growth defect, we transformed a *trf4ts top1*Δ double mutant with *cid14*$^+$ under the control of a galactose-inducible promoter. As shown in Fig. 1A, *cid14*$^+$ complemented the temperature-sensitive growth phenotype of the *trf4ts top1*Δ double mutant. The double mutant containing vector alone grew at 25°C but was unable to grow at 36°C. Expression of *TRF4* or *cid14*$^+$ but not *cid1*$^+$ was able to support growth of the double mutant at both temperatures. We conclude that the *S. pombe cid14*$^+$ and *S. cerevisiae TRF4* genes are functionally homologous. Multiple sequence comparisons suggest that *TRF4* and *TRF5* were generated by a relatively recent gene duplication event, so it is likely that the single *cid14* gene performs the *TRF4/5*-like function in *S. pombe*. Consistent with this hypothesis, no synthetic lethality was ob-

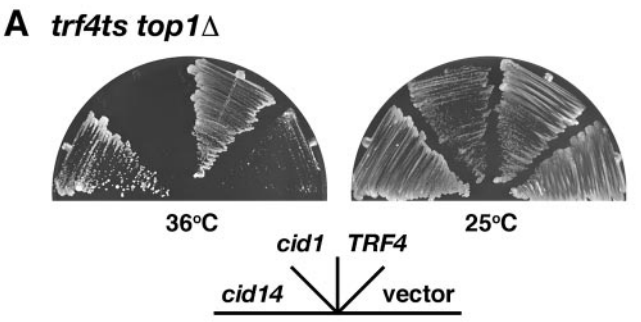

Sequence homology/similarity between Trf4, Trf5 and Cid proteins

	Cid1	Cid12	Cid13	Cid14
Trf4	26/42	27/49	22/42	36/57
Trf5*	21/49	25/44	23/44	35/56

*Trf5 sequence is 58% identical and 72% similar to Trf4

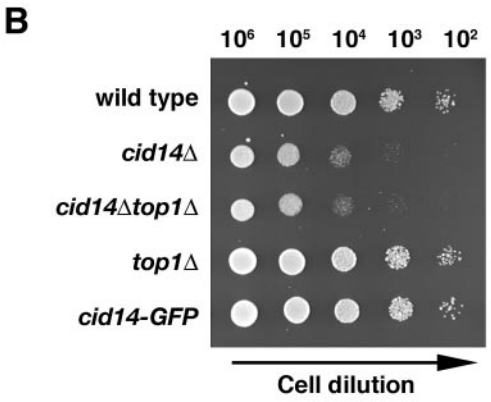

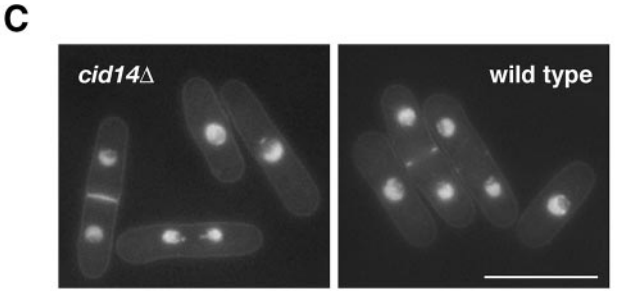

FIG. 1. *S. pombe cid14* is a functional homologue of *S. cerevisiae TRF4* and is required for normal cell growth. (A) *trf4ts top1*Δ mutants transformed with plasmids carrying full-length *cid1*, *cid14*, and *TRF4*, as indicated, under the control of the *GAL1* promoter or "empty" vector were streaked onto synthetic defined plates containing galactose. Plates were photographed after 3 days of incubation at 25°C or the nonpermissive temperature of 36°C. (B) Tenfold serial dilutions of the indicated strains spanning the range from 10^6 to 10^2 cells, as indicated, were spotted onto YE-agar plates and photographed after 2 days of incubation at 30°C. (C) Micrographs of Hoechst 33342-stained living wild-type and *cid14*Δ cells. Bar: 10 μm.

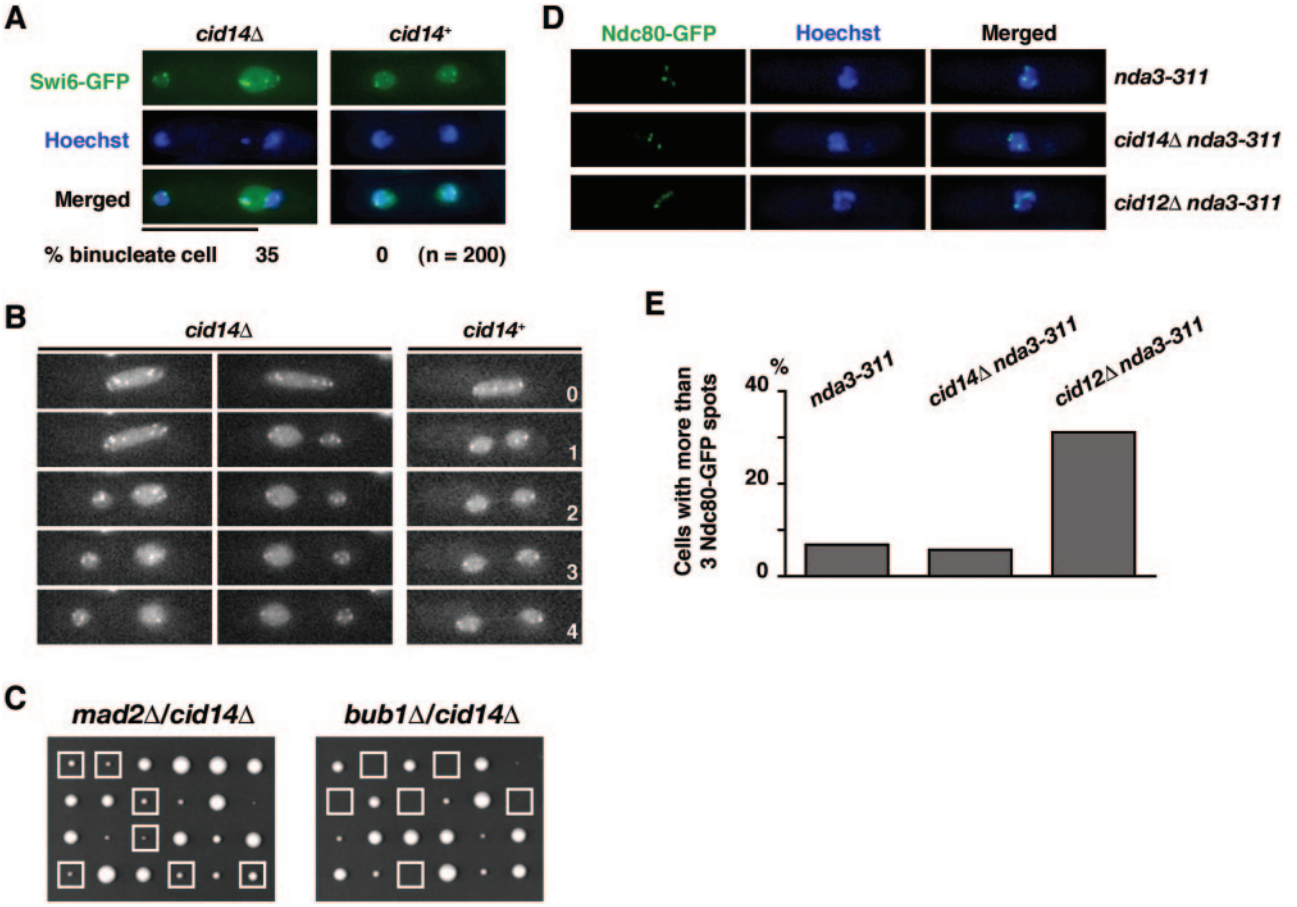

FIG. 2. Deletion of *cid14* leads to an increased chromosome segregation failure rate but not to precocious sister chromatid separation during metaphase arrest. (A) Merged images of fluorescence micrographs showing GFP-Swi6 and DNA (Hoechst 33342) localization in living cells. Bar: 10 μm. Percentages of cells with lagging chromosomes are indicated. (B) Visualization of unequal segregation of GFP-Swi6 signal in *cid14*Δ cells. Individual *GFP-swi6* (*cid14*$^+$) and *GFP-swi6 cid14*Δ cells were observed as for panel A, over a 4-min period, with images collected every minute. (C) Six tetrads derived from diploid strains h^+/h^- *mad2*::*ura4*$^+$/*mad2*$^+$ *cid14*::*LEU2*/*cid14*$^+$ (left) and *bub1*::*ura4*$^+$/*bub1*$^+$ *cid14*::*LEU2*/*cid14*$^+$ (right) were microdissected onto YE-agar, and the resulting colonies were photographed after 5 days of growth at 30°C. The genotypes of the segregants were determined by replica plating. Boxes indicate the position of *cid14* double mutants with *mad2* and *bub1*, respectively. (D) Merged images of fluorescence micrographs showing Ndc80-GFP localization in *nda3-KM311*, *cid14*Δ *nda3-KM311*, and *cid12*Δ *nda3-KM311* cells in EMM medium after incubation at 20°C for 8 h. Fluorescence micrographs of living cells were acquired after staining with Hoechst 33342, revealing green fluorescence (Ndc80-GFP) and DNA (Hoechst). (E) Percentages of cells with more than three Ndc80-GFP spots, indicative of precocious sister chromatid separation, in each strain are shown (n = 200).

served in *cid14*Δ mutants in combination with deletion of any other *cid* genes (data not shown).

***S. pombe cid14* is not essential for mitotic growth.** The one-step gene disruption method was used in a *ura4*$^-$/*ura4*$^-$ diploid *S. pombe* strain to replace one copy of the entire *cid14* open reading frame with the *ura4*$^+$ selectable marker. After induction of meiosis and sporulation, microdissection of tetrads showed that *cid14*::*ura4*$^+$ alleles segregated 2:2, indicating that, in contrast to its *S. cerevisiae* orthologue pair *TRF4*/*5*, *S. pombe cid14*$^+$ is not essential for mitotic growth despite the slow-growth phenotype (Fig. 1B). This phenotype was most marked in cells growing in liquid minimal medium in which *cid14*Δ cells grew with a doubling time of approximately 9 h, compared with 2.5 h for a *cid14*$^+$ strain. In addition, unlike *trf4* and *trf5* mutants, *cid14* deletion mutants remained fully viable on mutation of *top1*, which encodes the fission yeast topoisomerase I (41). Microscopic examination showed that *cid14*Δ cells retained an essentially normal morphology as judged by cell staining to reveal distribution of DNA, septa, and actin (Fig. 1C and data not shown).

Deletion of *cid14* leads to an increased chromosome segregation failure rate but not precocious sister chromatid separation during metaphase arrest. In *S. cerevisiae* Trf4 was reported to be required for the establishment of sister chromatid cohesion during S phase to ensure faithful chromosome segregation at mitosis (47). We therefore asked whether or not Cid14 is required for faithful chromosome segregation. To address this point, wild-type and *cid14*Δ strains containing an integrated GFP-tagged *swi6* gene were constructed. GFP-Swi6 is localized in the nucleoplasm, giving a background of faint nuclear signal and several brightly fluorescent spots corresponding to the heterochromatic centromeres and telomeres (28). As shown in Fig. 2A and B, anaphase chromosome segregation in living cells as monitored by GFP-Swi6 fluorescence

appeared normal in the *cid14*$^+$ background. In contrast, abnormal anaphase progression (segregation of two unequal masses of GFP-Swi6) was observed in 35% of binucleate *cid14*Δ cells. Consistent with these apparent chromosome segregation defects, *cid14*Δ mutants had a moderate increase in the rate of minichromosome loss. Mean loss rates were 0.14% and 0.04% per division for *cid14*Δ and wild-type strains, respectively (average of three independent clones), using strains containing the nonessential *ade6-M216*-marked Ch16 minichromosome derivative of chromosome 3 (25). Despite the chromosome segregation defects described, *cid14*Δ mutants are viable, indicating that the spindle checkpoint might be required for the survival of these cells. Indeed, as shown in Fig. 2C, deletion of *bub1* (4) but not *mad2* (10) is lethal in *cid14*Δ cells, indicating that a subset of the spindle checkpoint factors are required for the survival of *cid14*Δ cells.

To test whether the observed chromosome segregation defects are due to defects in sister chromatid cohesion, we monitored sister centromere separation by the use of a strain expressing a GFP-tagged version of the kinetochore component Ndc80 (49). Ndc80-GFP appears as a single fluorescent spot in interphase cells, while in anaphase the clustered kinetochores are seen as two spots, one in each daughter nucleus. When this strain was arrested in metaphase by inactivation of *nda3* (11), a mutation affecting β-tubulin, most cells (63%) still showed a single Ndc80-GFP spot, indicating that the sister centromeres were clustered. The remaining cells had three well-defined masses of condensed chromatin, presumably corresponding to the three *S. pombe* chromosomes, with Ndc80-GFP associated with each (Fig. 2D). This pattern of Ndc80-GFP distribution was seen in *nda3-KM311 cid14*Δ cells after shifting to the restrictive temperature to induce arrest at metaphase (Fig. 2E). In contrast, cells displaying separated Ndc80-GFP signals (more than three spots) were dramatically increased in a *cid12*Δ mutant defective in centromeric cohesion mediated by the RNA interference machinery (24). Thus, unlike *S. cerevisiae trf4* mutants, *S. pombe cid14*Δ cells showed no indication of premature sister centromere separation during metaphase arrest.

Characterization of Cid14 protein in *S. pombe*. Targeted recombination was used to add an HA epitope tag sequence to the 3′ end of the *cid14* open reading frame in its normal chromosomal context, generating the *cid14-HA* strain. Western blot analysis showed that the Cid14 protein had an aberrant mobility when analyzed by SDS-PAGE. While the calculated molecular mass of the protein is 78 kDa, the Cid14 protein isolated from *S. pombe* cells migrated as a predominant band of approximately 100 kDa (Fig. 3A). Next, we examined the expression of the Cid14 protein during the cell cycle. For this, *cdc25-22 cid14-HA* cells, released synchronously after cell cycle arrest at the restrictive temperature, were collected every 25 min and their lysates were subjected to immunoblotting. Cell cycle synchrony and position were monitored by determining the septation index. As shown in Fig. 3B, the Cid14 protein level remains constant with no obvious mobility shift through the cell cycle. Recently, *S. cerevisiae* Trf4 was reported to function in a complex with Mtr4 and Air1/2 (21, 40, 51). To determine whether or not Cid14 also functions as part of a higher-order complex, we used gel filtration chromatography to examine the native size of *S. pombe* Cid14 in a cell lysate prepared from the *cid14-HA* strain. As shown in Fig. 3C, the cellular Cid14 protein was found to be almost exclusively included in a large complex with an apparent size between 669 and 2,000 kDa. This result indicates that Cid14, like Trf4, forms part of a large complex in vivo.

***S. pombe* Cid14 is a nuclear protein enriched in the nucleolus.** To monitor the localization of Cid14 in living cells, the one-step gene replacement method was used to generate a strain (*cid14-GFP*) encoding a C-terminally GFP-tagged version of Cid14. The GFP-tagged protein appeared to be functional, as judged by the normal growth of the *cid14-GFP* strain compared with the *cid14*Δ strain (Fig. 1B). Examination of living *cid14-GFP* cells by fluorescence microscopy showed that Cid14-GFP (and, by inference, Cid14) was predominantly localized to the nucleus and was concentrated in a condensed spot in the nonchromosomal domain (Fig. 3D), previously assigned as the nucleolus (39). This phenomenon was further explored by examination of Cid14-GFP localization in an *nda3-KM311* mutant in which chromosomes condense after incubation at the restrictive temperature of 20°C for 8 h. As shown in Fig. 3E, the intense fluorescence of Cid14-GFP signal was associated with the smallest chromosome, consistent with the fact that the shortest *S. pombe* chromosome (III) contains the rRNA gene clusters. In line with these results, Cid14 colocalized with the region of intense ethidium bromide staining (Fig. 3F), which distinguishes the nucleolus from the rest of the nucleus (38). The nucleolar concentration of Cid14-GFP was observed in cells from all stages of the cell cycle (Fig. 3D).

Aberrant nucleolar structures in *cid14* mutants. Next, we asked whether or not Cid14 deficiency might affect nucleolar architecture. Nucleolar structure was visualized in living cells using a protein that was a fusion between GFP and the nucleolar protein Gar2 (34). In wild-type cells, Gar2-GFP occupied roughly one-half of the nucleus, in a discrete region distinct from the bulk chromosomal DNA, against a background of fainter nuclear signal (Fig. 4A, lower panels). In contrast, a more diffuse Gar2-GFP fluorescence signal was observed in the majority of *cid14*Δ cells (examples 1 to 3) and, upon entry into mitosis, these cells often failed to segregate Gar2-GFP properly (example 4). This phenomenon was further explored by time-lapse microscopy. As shown in Fig. 4B, in contrast to wild-type cells, in which Gar2-GFP separated equally into the daughter cells at mitosis, abnormal anaphase progression (segregation of two unequal masses of Gar2-GFP) frequently occurred in *cid14*Δ cells. Taken together, these results suggest that Cid14 might play a role in the organization of the nucleolus to ensure faithful segregation during mitosis.

Cid14-dependent polyadenylated rRNAs are accumulated in a *dis3-54* mutant. We reasoned that, given its cellular localization and requirement in the maintenance of nucleolar structure, Cid14 might have a role in rRNA metabolism through its predicted polyadenylation activity. In contrast to mRNA, rRNAs are not generally considered to be polyadenylated because they lack recognizable polyadenylation signals and are not synthesized by RNA polymerase II. However, recent data seriously undermine this notion by demonstrating that, in *S. cerevisiae*, some rRNAs can indeed be polyadenylated (9, 19). To explore whether Cid14 polyadenylates rRNA, we examined the 3′ end of the 25S rRNA using a RACE-PAT assay (32). As shown in Fig. 5C, distinct products of lengths consistent with

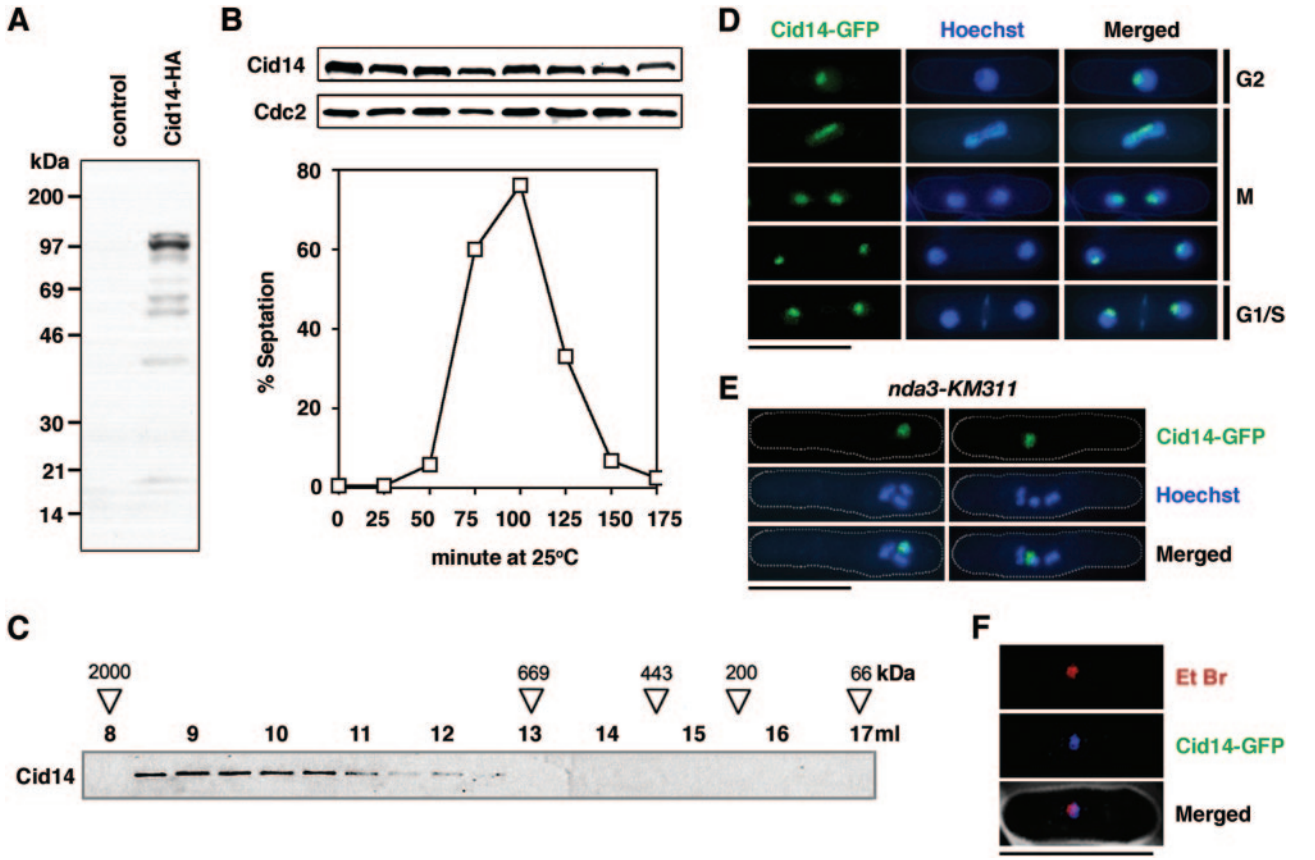

FIG. 3. *S. pombe* Cid14 localizes to the nucleolus throughout the cell cycle. (A) Whole-cell protein extracts from wild-type (control) and *cid14-HA* strains were prepared by trichloroacetic acid precipitation following glass bead disruption. The extracts were separated by SDS-PAGE and subjected to immunoblotting using anti-HA antibodies. (B) Cells expressing Cid14-HA were synchronously released from the G_2 block imposed by a temperature-sensitive *cdc25-22* mutation. Samples taken at the times indicated were used to score percentages of septated cells and subjected to immunoblotting using anti-HA (Cid14) or anti-Cdc2 (loading control) antibodies as indicated. (C) The size of soluble Cid14-HA was estimated by gel filtration chromatography. Samples of each 0.5-ml Superose-6 column fraction were processed for immunoblotting with an anti-HA antibody. The elution volume (ml) of each fraction is shown above the blots. The positions at which dextran blue (~2,000 kDa), thyroglobulin (669 kDa), apoferritin (443 kDa), β-amylase (200 kDa), and bovine serum albumin (66 kDa) migrated are indicated. (D and E) Merged images of fluorescence micrographs showing Cid14-GFP and DNA (Hoechst 33342) localization in (D) living wild-type cells grown at 30°C and (E) *nda3-KM311* mutants after incubation at 20°C for 8 h. (F) Merged images of fluorescence micrographs showing Cid14-GFP and nucleolar localization (Et Br, ethidium bromide) in living cells grown at 30°C. Bar: 10 μm.

polyadenylation in the region of the mature 25S rRNA 3′ end were observed in wild-type cells that were not detected in the "no-RT" control. The PCR-amplified products were cloned and sequenced. Each of 11 randomly selected clones contained a poly(A) sequence 12 to 48 nucleotides long immediately downstream of the mature 3′ end of the 25S rRNA, which is generated in several steps by posttranscriptional processing during rRNA biogenesis (Fig. 5B). There is no templated poly(A) tract in this region, suggesting that the poly(A) detected in this assay was not due to nonspecific priming. We conclude that rRNA can contain 3′ poly(A) tails in *S. pombe*.

To estimate the relative levels of polyadenylated 25S rRNA, the levels of these products were compared with a series of RT-PCR assays performed on diluted samples of the same RNAs (Fig. 5E). This analysis showed that the polyadenylated 25S rRNA product is approximately 0.02% of total 25S rRNA in wild-type cells. Consistent with a role for the exosome in rRNA processing and degradation, the polyadenylated 25S rRNA products were accumulated in a *dis3*/*RPR44* exosome mutant and increased further after 8 h of incubation at the nonpermissive temperature of 20°C (Fig. 5C). The amounts of mature 18S and 25S rRNAs were very similar in all cell types examined (Fig. 5C and E), indicating that cleavage steps were not adversely affected by the mutations. These results are consistent with a model in which a polyadenylation-assisted degradation mechanism is responsible for the degradation of aberrant RNA transcripts. Furthermore, these polyadenylated 25S rRNA products were not detectable in the *cid14*Δ and *cid14*Δ *dis3-54* strains, suggesting that Cid14 plays a role in adenylating the rRNAs. In line with its predicted polyadenylation activity, the polyadenylated 25S rRNA products were found to be dependent on the conserved aspartate residues 298 and 230 in the nucleotide transferase motif (GS X_{10} DXD) of Cid14 that are known to be essential for the catalytic activity of this protein family (Fig. 5D). When expressed in the *cid14*Δ strain from the *nmt1* promoter in the plasmid pREP1*cid14DADA* in the pres-

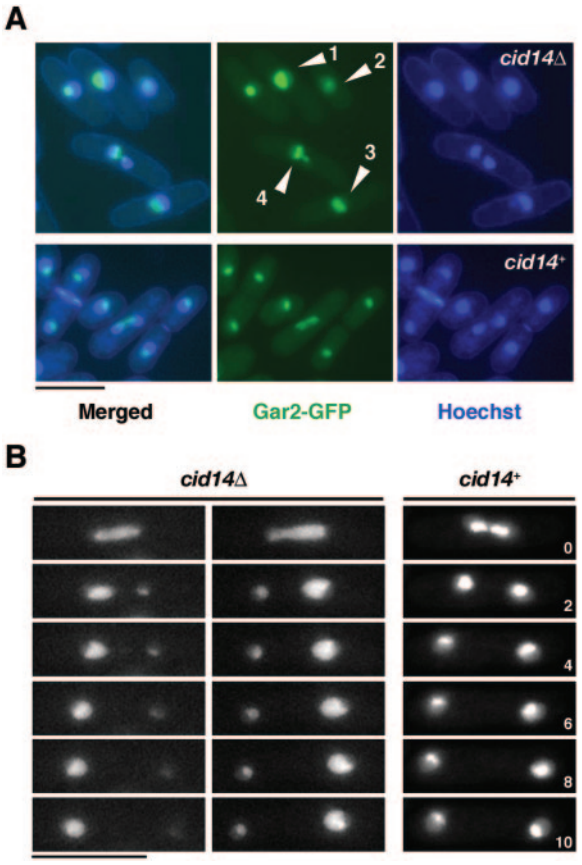

FIG. 4. Aberrant nucleolar structures in the *cid14*Δ mutants. (A) Merged images of fluorescence micrographs showing Gar2-GFP and DNA (Hoechst 33342) localization in living cells. Arrowheads indicate cells with aberrant nucleolar structures. (B) Visualization of unequal segregation of Gar2-GFP signal in *cid14*Δ cells. Individual *gar2-GFP* (*cid14*$^+$) and *gar2-GFP cid14*Δ cells were observed as in panel A, over a 10-min period, with images collected every 2 min. Bar: 10 μm.

ence of thiamine, this mutant form of Cid14, unlike the wild-type protein, was unable to restore the polyadenylated 25S rRNA species in these cells.

Next, we asked whether or not the other three types of rRNA might be polyadenylated and accumulate in a *dis3-54* mutant. As shown in Fig. 6A, similar results were observed in the RACE-PAT assay of 5.8S RNA. Sequencing analysis confirmed Cid14-dependent polyadenylation of 5.8S RNAs, as these products were dramatically reduced in the *cid14*Δ and *cid14*Δ *dis3-54* strains. The residue products presented in *cid14*Δ cells were due to nonspecific priming as confirmed by sequencing of 17 randomly selected clones (data not shown). No obvious difference was observed in the amount of these polyadenylated 5.8S rRNA products in *dis3-54* mutants compared with the wild-type strain. Although it has been reported that 18S RNAs are polyadenylated to a certain level (19), we were not able to detect any polyadenylated 18S rRNA products using an approach similar to that described above (data not shown).

In contrast to the genes for the large rRNAs, the 5S gene sequences are dispersed within the genome and are transcribed by RNA polymerase III independently of other rRNA genes. As shown in Fig. 6E, RACE-PAT assays identified two forms of polyadenylated 5S rRNA products. A broad band of longer transcripts with poly(A) tails downstream of the mature 3′ end of 5S rRNA was observed in all strains examined. Interestingly, deletion of *cid14* had no influence on the amount of these transcripts, in sharp contrast to what we observed for the 5.8S and 25S genes. In addition, a band of shorter products which contained fragments of 5S RNAs with poly(A) tails (gray arrowheads in Fig. 6F) were detected only in the *dis3-54* cells. The dependence of these products on *dis3* mutation implied that these molecules were destined for exosome-mediated degradation. Consistent with a role of Cid14 in polyadenylation-assisted degradation, the polyadenylated 5S-related RNAs were not detectable in the *cid14*Δ *dis3-54* strain.

In line with these results, *cid14*Δ cells were hypersensitive to 5-fluorouracil (5-FU; Fig. 6G), a chemical which interferes with the degradation of rRNA precursors (9).

Deletion of *cid14* leads to stimulation of meiosis in *pat1-114* cells. In *C. elegans*, the Cid1-related protein GLD-2 together with its RNA binding partner GLD-3 controls various aspects of germ line development, including the mitosis/meiosis decision (42), while in *Xenopus* xGLD-2 is required for CPEB-mediated polyadenylation-induced translation during oocyte maturation (3). We were therefore interested to see whether or not Cid14 plays a role in meiosis in fission yeast. To test this, we examined the genetic interaction between *cid14* and *pat1*, which encodes a general inhibitor of sexual differentiation (22). As shown in Fig. 7A and B, whereas the *pat1-114* single mutants enter meiosis at 30°C, the *pat1-114 cid14*Δ mutants initiated meiosis at the normally permissive temperature of 25°C. Similarly, *pat1-114 dis3-54* mutants underwent meiosis at the lower temperature. These results suggest that Cid14 together with the exosome might play a role in meiosis, closely interacting with the Pat1 kinase.

In *S. pombe*, the switch from mitosis to meiosis is controlled by the Pat1 kinase-Mei2 system. Mei2, an RNA-binding protein, is essential for the initiation of premeiotic DNA synthesis and meiosis I (48). Transcription of *mei2* is activated by nutrient deprivation and a concomitant decrease in the intracellular cyclic AMP level and is directly regulated by Ste11, which is a transcription factor of the high-mobility-group family (36). During the normal mitotic cycle, Pat1 suppresses meiotic entry via transcriptional repression through Ste11, in addition to the direct inhibition of Mei2 by phosphorylation (18). To understand the role of Cid14 in meiotic control, we measured the levels of *ste11* and *mei2* mRNAs in *cid14*Δ cells as well as in *dis3-54* mutants grown at the permissive temperature 30°C. As shown in Fig. 7C, deletion of *cid14*, or *dis3* mutation, led to accumulation of *mei2* transcripts as determined by quantitative PCR. Mutation of *dis3* also affected the *stell* mRNA level. The elevated levels of *mei2* mRNA could account for the stimulation of meiosis in *pat1-114 cid14*Δ and *pat1-114 dis3-54* cells.

DISCUSSION

The Cid1 family of nucleotidyltransferases is widespread in eukaryotes (20). Members of this family (Cid1 and Cid13 in fission yeast and GLD-2 in *C. elegans* and vertebrates) have been shown to use RNA substrates and define a cytoplasmic

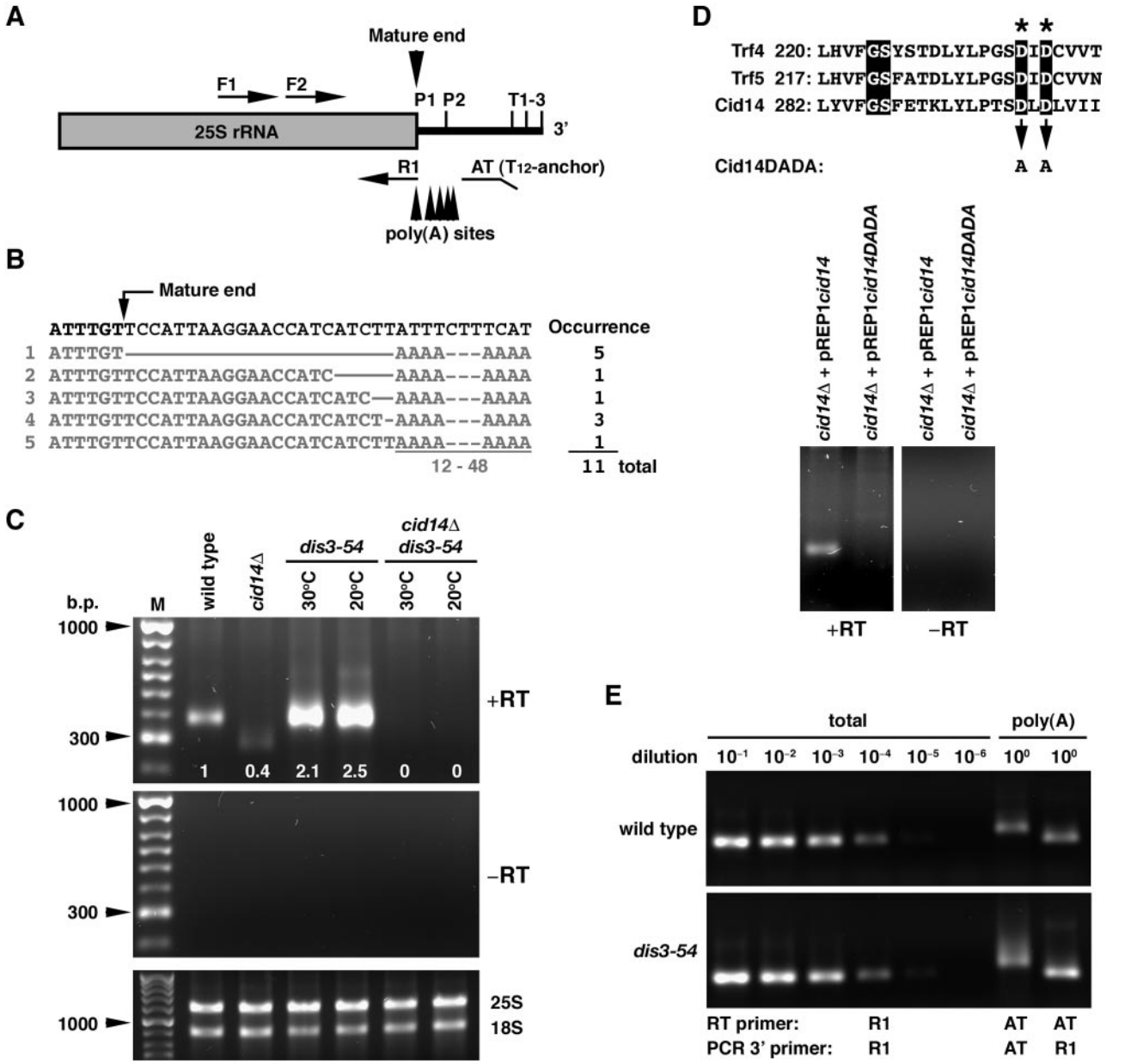

FIG. 5. Cid14-dependent polyadenylated 25S rRNAs are accumulated in a *dis3-54* mutant. (A) Schematic diagram of the primers for RT-PCR. Alternative processing cleavage sites (P1 and P2) and transcription termination sites (T1-3) are indicated. (B) The 3′-terminal sequences of cloned reverse transcription products. (C) Total RNA from cultures of indicated strains grown at 30°C or the nonpermissive temperature of 20°C for *dis3-54* mutants was reverse transcribed using the anchored oligo(dT) primer AT and then PCR amplified with AT and the F1 primer specific for 25S rRNA. RT-PCR products were separated on a 1% agarose gel, and the relative signals were quantified as indicated. A control using total RNA and a non-reverse-transcribed negative control were included. (D) Total RNA from cultures of *cid14*Δ strains containing the indicated plasmids (with or without mutation in the nucleotide transferase motif: GS X_{10} DXD of Cid14) and grown in the presence of 15 μM thiamine was subjected to RACE-PAT assay as for panel C. RT-PCR products were separated on a 1% agarose gel. A non-reverse-transcribed negative control was included. (E) Reverse transcripts were made with the R1 or AT primer and RNA from wild-type and *dis3-54* strains grown at 30°C. Serial dilutions of R1 transcripts (for total 25S rRNA) were PCR amplified with F2 and R1 and compared with AT transcripts (polyadenylated 25S rRNA) amplified with primer pair F2 and AT or F2 and R1.

family of poly(A) polymerases (29, 31, 42). In contrast, the *S. cerevisiae* Cid1-related protein Trf4 was identified as a component of a nuclear polyadenylation complex and is required for polyadenylation and degradation of rRNA and snoRNA precursors that are characterized as exosome substrates (21, 51). In this study, we have identified Cid14 as the functional homologue of *S. cerevisiae* Trf4/5. We have provided evidence suggesting that in *S. pombe* subpopulations at least three of the four rRNAs contain 3′ poly(A) tails and, at some level, Cid14 appears responsible for the polyadenylation of these rRNAs. It has been proposed that polyadenylation by the Trf4 complex stimulates RNA degradation by the exosome. Consistent with

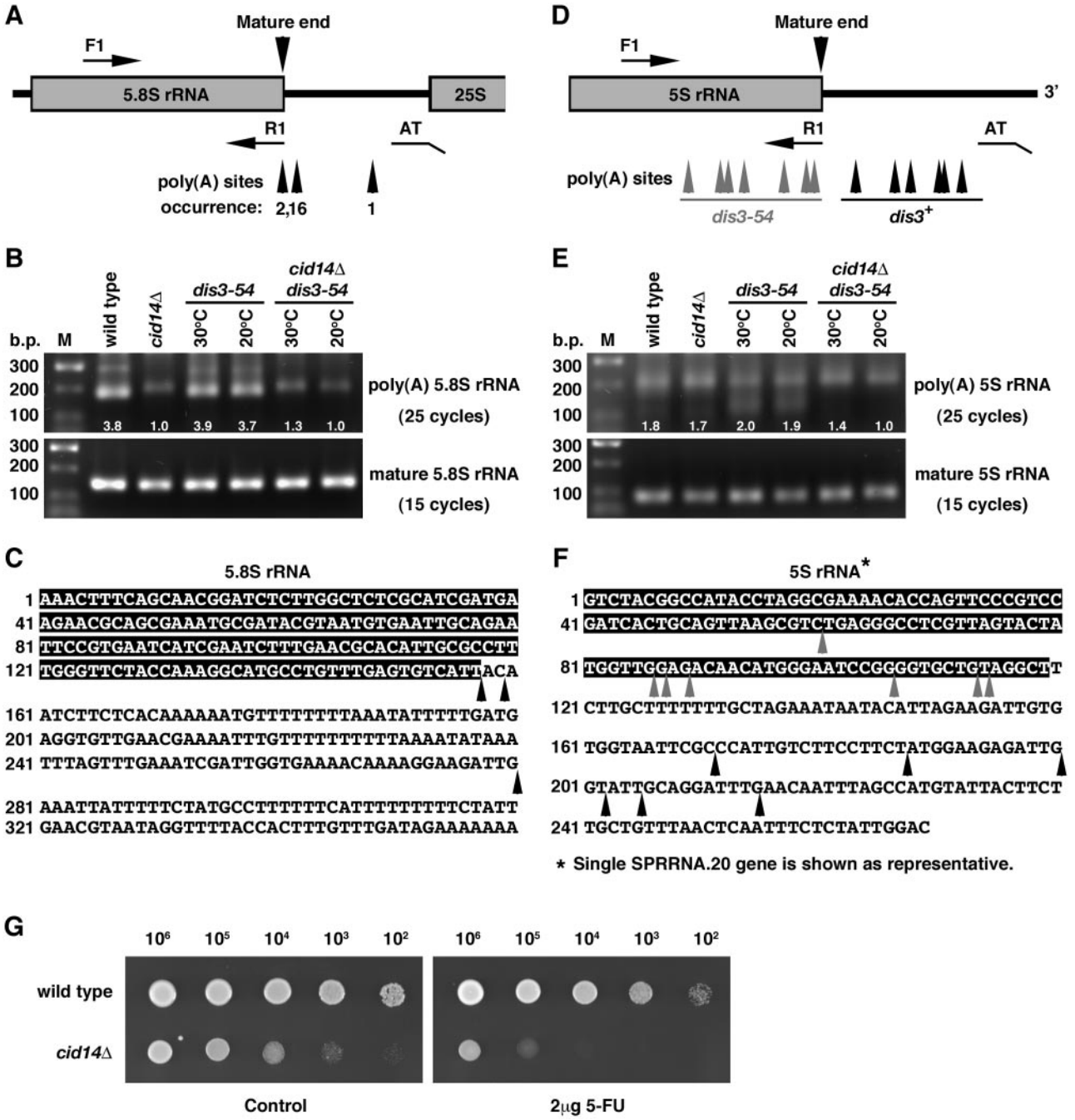

FIG. 6. Analysis of the polyadenylation status of 5.8S and 5S rRNA in different genetic backgrounds. (A and D) Schematic diagram of the primers for RT-PCR. (B and E) Total RNA from cultures of indicated strains grown at 30°C or the nonpermissive temperature of 20°C for *dis3-54* mutants was reverse-transcribed with the oligo(dT) anchor primer AT and then PCR amplified with AT and forward primers F1 specific for 5.8S and 5S rRNA, respectively. For detection of mature rRNA, reverse transcripts were made with the R1 primer specific for 5.8S and 5S rRNA and then PCR amplified with pair F1 and R1. RT-PCR products were separated on a 1.5% agarose gel, and the relative signals were quantified as indicated. (C and F) Genomic sequences of 5.8S and 5S genes. Arrowheads indicate polyadenylation sites identified. (G) Tenfold serial dilutions of wild-type and *cid14*Δ strains spanning the range from 10^6 to 10^2 cells, as indicated, were spotted onto YE-agar containing 2 μg/ml 5-FU or no drug (control). Plates were photographed after 3 days of incubation at 30°C.

this hypothesis, the Cid14-dependent polyadenylated rRNAs were accumulated in a *dis3* mutant defective in a component of the exosome. In addition, our results also revealed a fraction of the polyadenylated rRNA species that are not dependent on Cid14 (Fig. 6E). In the absence of Cid14, an alternative pathway must be responsible for the polyadenylation of these rRNAs; low levels of polyadenylated 25S rRNA products with alternative polyadenylation sites were observed in *cid14*Δ mutants (data not shown). It has been reported that polyadenylation of several rRNA species in a *rrp6*Δ background depends

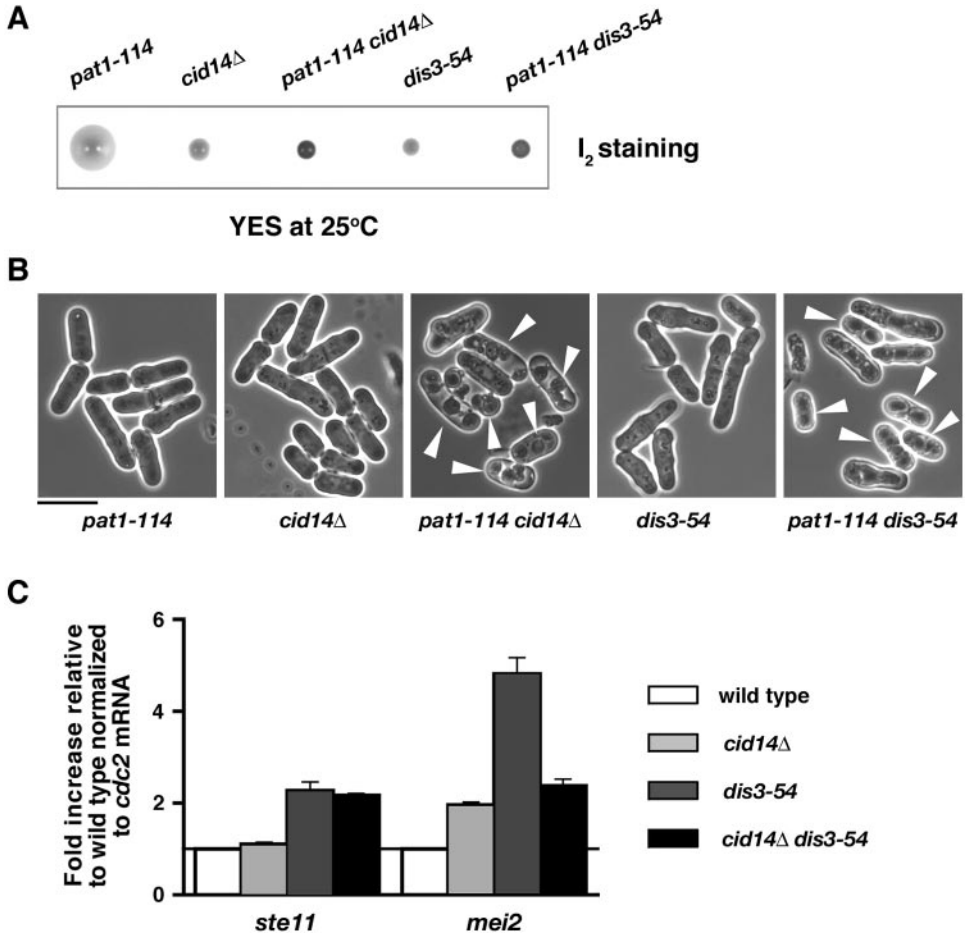

FIG. 7. Deletion of *cid14* leads to stimulation of meiosis in *pat1-114* cells. (A) Iodine staining of colonies derived from spores of diploid h^+/h^- *cid14*::*ura4*$^+$/*cid14*$^+$ *pat1-114*/*pat1*$^+$ and h^+/h^- *dis3-54*/*dis3*$^+$ *pat1-114*/*pat1*$^+$ strains after 5 days of growth on YE-agar at 25°C. Iodine stains cells that have undergone meiosis and sporulation dark brown. (B) Micrographs of the strains indicated from panel A. Arrowheads indicate cells that have undergone meiosis and sporulation. Bar: 10 μm. (C) Total RNA from cultures of the indicated strains grown at 30°C was reverse transcribed using an oligo(dT) primer. The cDNA was amplified using quantitative PCR and SYBR green in triplicate with primers specific for the indicated genes. RNA amounts normalized to *cdc2* mRNA were expressed relative to the wild type.

on the nuclear poly(A) polymerase (19, 51). Whether or not Pla1, the canonical *S. pombe* poly(A) polymerase, is responsible for the polyadenylation of these transcripts remains to be determined. However, the significance of polyadenylation of these transcripts is unclear; it does not appear to stimulate their degradation by the exosome, as the mutation of *dis3* has no influence on the amount of these transcripts. In line with these results, cells that lack a functional *cid14*$^+$ gene grow slowly and are hypersensitive to 5-FU (Fig. 6G).

Consistent with its role in rRNA metabolism, *S. pombe* Cid14 is a nucleolar protein and is required for maintenance of nucleolar structure (Fig. 3 and 4). Similarly, Dis3 protein (and, by inference the exosome) is enriched in the nucleolus (17). Intriguingly, polyadenylation of 5S rRNAs, transcribed by RNA polymerase III outside the nucleolus, is also dependent on Cid14 to a degree (Fig. 6). This could be due to the function of nucleolus in the processing of rRNAs and their subsequent assembly into preribosomes. The fact that a Trf4-dependent polyadenylation-assisted degradation mechanism is also responsible for the degradation of RNA polymerase II transcripts (51) broadens the implication of these results. Possible involvement of the nucleolus in mRNA export has been proposed, based on observations made in yeasts and higher eukaryotic cells (5, 8, 13, 33). These results suggest that the nucleolus might function as a site of general RNA quality control, although it is still unclear how the cell determines which transcripts should be degraded.

Chromosome segregation defects were another obvious feature of *cid14*-deficient cells (Fig. 2). In *S. cerevisiae* Trf4 was reported to be required for the establishment of sister chromatid cohesion during S phase to ensure faithful chromosome segregation at mitosis (47). However, unlike *S. cerevisiae Trf4* mutants, *S. pombe cid14*Δ cells showed no indication of premature sister centromere separation during metaphase arrest (Fig. 2D and E). Given the function of Cid14 in rRNA metabolism, ribosome biogenesis and translation defects might have a direct effect on some aspect of chromosome structure or kinetochore function. Alternatively, the impact of a loss of Cid14 function in mitosis may be through impaired expression of genes required for faithful chromosome segregation. In-

triguingly, in *S. pombe*, the *dis3*$^+$ gene was first identified through a screen for mutants defective in mitotic chromosome separation (17, 26, 27). The same screen identified *dis2*$^+$, which encodes a serine-threonine protein phosphatase identified as a component of the pre-mRNA cleavage and polyadenylation complex (30). Similar defects have been reported for *pfs2* mutants, which are defective in another component of the pre-mRNA cleavage and polyadenylation complex (43). The characterization of *S. pombe* mutants defective in the 5′-3′ exoribonuclease Dhp1 suggested an additional connection between RNA processing and chromosome segregation (35). It will be interesting to determine whether or not chromosome segregation defects are a general feature of mutants defective in RNA processing.

Our results also revealed a possible function of Cid14 in the control of meiosis. In *C. elegans*, the Cid1-related protein GLD-2 promotes entry into meiosis from the mitotic cell cycle (16). In contrast, deletion of *cid14* leads to stimulation of meiosis in *pat1-114* cells (Fig. 7). This effect could be due to the deprivation of nutrients as a consequence of defective ribosome biogenesis. However, *pat1-144* cells arrested at G_1 rather than entering meiosis after deprivation of nutrients by nitrogen starvation at the permissive temperature 25°C (data not shown). These results suggest that Cid14 together with the exosome might have a more direct role in meiotic control. Additional connections between RNA processing and meiosis were suggested by the identification of *S. pombe pac1*$^+$, which encodes an RNase III-like RNase, as a multicopy suppressor of the uncontrolled meiosis driven by *pat1* deficiency (14). The *pac1* gene product probably inhibits mating and meiosis by degrading mRNAs required for sexual development. The accumulation of mRNAs required for meiosis in exosome mutants suggests that these transcripts might be constantly degraded by the exosome in mitotic cells to prevent ectopic meiosis. Experiments are under way to explore this possibility.

Cid1-like proteins control a variety of functions in *S. pombe*, *C. elegans*, and vertebrates. The identification of Cid14 as the functional homologue of *S. cerevisiae* Trf4/5 indicates the generality of a polyadenylation-assisted degradation mechanism, which is likely to be conserved in higher eukaryotes. Interestingly, in contrast to the situation in other organisms, no cytoplasmic function of Trf4/5 has been described. Studying the way in which Cid1-like proteins function in lower eukaryotes is expected to provide greater understanding of the biological functions of polyadenylation in eukaryotic cells in general.

ACKNOWLEDGMENTS

We thank Michael F. Christman, Jean-Paul Javerzat, Nancy C. Walworth, Mitsuhiro Yanagida, and Masayuki Yamamoto for yeast strains; Hiro Yamano for Cdc2 antibody; and Stephen Kearsey for useful discussions and comments on the manuscript.

This work was supported by Cancer Research UK and The Wellcome Trust (Research Career Development Fellowship to Shao-Win Wang).

REFERENCES

1. **Allshire, R. C., E. R. Nimmo, K. Ekwall, J. P. Javerzat, and G. Cranston.** 1995. Mutations derepressing silent centromeric domains in fission yeast disrupt chromosome segregation. Genes Dev. **9:**218–233.
2. **Ausubel, F. M., R. Brent, R. E. Kingston, D. D. Moore, J. G. Seidman, J. A. Smith, and K. Struhl (ed.).** 1995. Current protocols in molecular biology. John Wiley and Son, Inc., New York, N.Y.
3. **Barnard, D. C., K. Ryan, J. L. Manley, and J. D. Richter.** 2004. Symplekin and xGLD-2 are required for CPEB-mediated cytoplasmic polyadenylation. Cell **119:**641–651.
4. **Bernard, P., K. Hardwick, and J. P. Javerzat.** 1998. Fission yeast bub1 is a mitotic centromere protein essential for the spindle checkpoint and the preservation of correct ploidy through mitosis. J. Cell Biol. **143:**1775–1787.
5. **Bond, V. C., and B. Wold.** 1993. Nucleolar localization of *myc* transcripts. Mol. Cell. Biol. **13:**3221–3230.
6. **Caspari, T., M. Dahlen, G. Kanter-Smoler, H. D. Lindsay, K. Hofmann, K. Papadimitriou, P. Sunnerhagen, and A. M. Carr.** 2000. Characterization of *Schizosaccharomyces pombe* Hus1: a PCNA-related protein that associates with Rad1 and Rad9. Mol. Cell. Biol. **20:**1254–1262.
7. **Castano, I. B., S. Heath-Pagliuso, B. U. Sadoff, D. J. Fitzhugh, and M. F. Christman.** 1996. A novel family of TRF (DNA topoisomerase I-related function) genes required for proper nuclear segregation. Nucleic Acids Res. **24:**2404–2410.
8. **Deak, I., E. Sidebottom, and H. Harris.** 1972. Further experiments on the role of the nucleolus in the expression of structural genes. J. Cell Sci. **11:**379–391.
9. **Fang, F., J. Hoskins, and J. S. Butler.** 2004. 5-Fluorouracil enhances exosome-dependent accumulation of polyadenylated rRNAs. Mol. Cell. Biol. **24:**10766–10776.
10. **He, X., T. E. Patterson, and S. Sazer.** 1997. The *Schizosaccharomyces pombe* spindle checkpoint protein mad2p blocks anaphase and genetically interacts with the anaphase-promoting complex. Proc. Natl. Acad. Sci. USA **94:**7965–7970.
11. **Hiraoka, Y., T. Toda, and M. Yanagida.** 1984. The NDA3 gene of fission yeast encodes beta-tubulin: a cold-sensitive nda3 mutation reversibly blocks spindle formation and chromosome movement in mitosis. Cell **39:**349–358.
12. **Huh, W. K., J. V. Falvo, L. C. Gerke, A. S. Carroll, R. W. Howson, J. S. Weissman, and E. K. O'Shea.** 2003. Global analysis of protein localization in budding yeast. Nature **425:**686–691.
13. **Ideue, T., A. K. Azad, J. Yoshida, T. Matsusaka, M. Yanagida, Y. Ohshima, and T. Tani.** 2004. The nucleolus is involved in mRNA export from the nucleus in fission yeast. J. Cell Sci. **117:**2887–2895.
14. **Iino, Y., A. Sugimoto, and M. Yamamoto.** 1991. *S. pombe pac1*$^+$, whose overexpression inhibits sexual development, encodes a ribonuclease III-like RNase. EMBO J. **10:**221–226.
15. **Kadaba, S., A. Krueger, T. Trice, A. M. Krecic, A. G. Hinnebusch, and J. Anderson.** 2004. Nuclear surveillance and degradation of hypomodified initiator $tRNA^{Met}$ in *S. cerevisiae*. Genes Dev. **18:**1227–1240.
16. **Kadyk, L. C., and J. Kimble.** 1998. Genetic regulation of entry into meiosis in *Caenorhabditis elegans*. Development **125:**1803–1813.
17. **Kinoshita, N., M. Goebl, and M. Yanagida.** 1991. The fission yeast *dis3*$^+$ gene encodes a 110-kilodalton essential protein implicated in mitotic control. Mol. Cell. Biol. **11:**5839–5847.
18. **Kitamura, K., S. Katayama, S. Dhut, M. Sato, Y. Watanabe, M. Yamamoto, and T. Toda.** 2001. Phosphorylation of Mei2 and Ste11 by Pat1 kinase inhibits sexual differentiation via ubiquitin proteolysis and 14-3-3 protein in fission yeast. Dev. Cell **1:**389–399.
19. **Kuai, L., F. Fang, J. S. Butler, and F. Sherman.** 2004. Polyadenylation of rRNA in *Saccharomyces cerevisiae*. Proc. Natl. Acad. Sci. USA **101:**8581–8586.
20. **Kwak, J. E., L. Wang, S. Ballantyne, J. Kimble, and M. Wickens.** 2004. Mammalian GLD-2 homologs are poly(A) polymerases. Proc. Natl. Acad. Sci. USA **101:**4407–4412.
21. **LaCava, J., J. Houseley, C. Saveanu, E. Petfalski, E. Thompson, A. Jacquier, and D. Tollervey.** 2005. RNA degradation by the exosome is promoted by a nuclear polyadenylation complex. Cell **121:**713–724.
22. **McLeod, M., and D. Beach.** 1988. A specific inhibitor of the ran1$^+$ protein kinase regulates entry into meiosis in *Schizosaccharomyces pombe*. Nature **332:**509–514.
23. **Moreno, S., A. Klar, and P. Nurse.** 1991. Molecular genetic analysis of fission yeast *Schizosaccharomyces pombe*. Methods Enzymol. **194:**795–823.
24. **Motamedi, M. R., A. Verdel, S. U. Colmenares, S. A. Gerber, S. P. Gygi, and D. Moazed.** 2004. Two RNAi complexes, RITS and RDRC, physically interact and localize to noncoding centromeric RNAs. Cell **119:**789–802.
25. **Niwa, O., T. Matsumoto, Y. Chikashige, and M. Yanagida.** 1989. Characterization of *Schizosaccharomyces pombe* minichromosome deletion derivatives and a functional allocation of their centromere. EMBO J. **8:**3045–3052.
26. **Noguchi, E., N. Hayashi, Y. Azuma, T. Seki, M. Nakamura, N. Nakashima, M. Yanagida, X. He, U. Mueller, S. Sazer, and T. Nishimoto.** 1996. Dis3, implicated in mitotic control, binds directly to Ran and enhances the GEF activity of RCC1. EMBO J. **15:**5595–5605.
27. **Ohkura, H., Y. Adachi, N. Kinoshita, O. Niwa, T. Toda, and M. Yanagida.** 1988. Cold-sensitive and caffeine-supersensitive mutants of the *Schizosaccharomyces pombe dis* genes implicated in sister chromatid separation during mitosis. EMBO J. **7:**1465–1473.
28. **Pidoux, A. L., S. Uzawa, P. E. Perry, W. Z. Cande, and R. C. Allshire.** 2000. Live analysis of lagging chromosomes during anaphase and their effect on spindle elongation rate in fission yeast. J. Cell Sci. **113**(Pt. 23)**:**4177–4191.
29. **Read, R. L., R. G. Martinho, S. W. Wang, A. M. Carr, and C. J. Norbury.**

2002. Cytoplasmic poly(A) polymerases mediate cellular responses to S phase arrest. Proc. Natl. Acad. Sci. USA **99:**12079–12084.
30. **Roguev, A., A. Shevchenko, D. Schaft, H. Thomas, and A. F. Stewart.** 2004. A comparative analysis of an orthologous proteomic environment in the yeasts *Saccharomyces cerevisiae* and *Schizosaccharomyces pombe*. Mol. Cell. Proteomics **3:**125–132.
31. **Saitoh, S., A. Chabes, W. H. McDonald, L. Thelander, J. R. Yates, and P. Russell.** 2002. Cid13 is a cytoplasmic poly(A) polymerase that regulates ribonucleotide reductase mRNA. Cell **109:**563–573.
32. **Salles, F. J., W. G. Richards, and S. Strickland.** 1999. Assaying the polyadenylation state of mRNAs. Methods **17:**38–45.
33. **Schneiter, R., T. Kadowaki, and A. M. Tartakoff.** 1995. mRNA transport in yeast: time to reinvestigate the functions of the nucleolus. Mol. Biol. Cell **6:**357–370.
34. **Shimada, T., A. Yamashita, and M. Yamamoto.** 2003. The fission yeast meiotic regulator Mei2p forms a dot structure in the horse-tail nucleus in association with the *sme2* locus on chromosome II. Mol. Biol. Cell **14:**2461–2469.
35. **Shobuike, T., K. Tatebayashi, T. Tani, S. Sugano, and H. Ikeda.** 2001. The *dhp1*$^+$ gene, encoding a putative nuclear 5′→3′ exoribonuclease, is required for proper chromosome segregation in fission yeast. Nucleic Acids Res. **29:**1326–1333.
36. **Sugimoto, A., Y. Iino, T. Maeda, Y. Watanabe, and M. Yamamoto.** 1991. *Schizosaccharomyces pombe ste11*$^+$ encodes a transcription factor with an HMG motif that is a critical regulator of sexual development. Genes Dev. **5:**1990–1999.
37. **Tomecki, R., A. Dmochowska, K. Gewartowski, A. Dziembowski, and P. P. Stepien.** 2004. Identification of a novel human nuclear-encoded mitochondrial poly(A) polymerase. Nucleic Acids Res. **32:**6001–6014.
38. **Umesono, K., Y. Hiraoka, T. Toda, and M. Yanagida.** 1983. Visualization of chromosomes in mitotically arrested cells of the fission yeast *Schizosaccharomyces pombe*. Curr. Genet. **7:**123–128.
39. **Uzawa, S., and M. Yanagida.** 1992. Visualization of centromeric and nucleolar DNA in fission yeast by fluorescence in situ hybridization. J. Cell Sci. **101**(Pt. 2)**:**267–275.
40. **Vanacova, S., J. Wolf, G. Martin, D. Blank, S. Dettwiler, A. Friedlein, H. Langen, G. Keith, and W. Keller.** 19 April 2005, posting date. A new yeast poly(A) polymerase complex involved in RNA quality control. PLoS Biol. *3:*e189. [Online.] http://biology.plosjournals.org/perlserv/?request=get-document&doi=10.1371/journal/pbio.0030189.
41. **Wan, S., H. Capasso, and N. C. Walworth.** 1999. The topoisomerase I poison camptothecin generates a Chk1-dependent DNA damage checkpoint signal in fission yeast. Yeast **15:**821–828.
42. **Wang, L., C. R. Eckmann, L. C. Kadyk, M. Wickens, and J. Kimble.** 2002. A regulatory cytoplasmic poly(A) polymerase in *Caenorhabditis elegans*. Nature **419:**312–316.
43. **Wang, S. W., K. Asakawa, T. Z. Win, T. Toda, and C. J. Norbury.** 2005. Inactivation of the pre-mRNA cleavage and polyadenylation factor Pfs2 in fission yeast causes lethal cell cycle defects. Mol. Cell. Biol. **25:**2288–2296.
44. **Wang, S. W., C. Norbury, A. L. Harris, and T. Toda.** 1999. Caffeine can override the S-M checkpoint in fission yeast. J. Cell Sci. **112**(Pt. 6)**:**927–937.
45. **Wang, S. W., R. L. Read, and C. J. Norbury.** 2002. Fission yeast Pds5 is required for accurate chromosome segregation and for survival after DNA damage or metaphase arrest. J. Cell Sci. **115:**587–598.
46. **Wang, S. W., T. Toda, R. MacCallum, A. L. Harris, and C. Norbury.** 2000. Cid1, a fission yeast protein required for S-M checkpoint control when DNA polymerase delta or epsilon is inactivated. Mol. Cell. Biol. **20:**3234–3244.
47. **Wang, Z., I. B. Castano, A. De Las Penas, C. Adams, and M. F. Christman.** 2000. Pol kappa: a DNA polymerase required for sister chromatid cohesion. Science **289:**774–779.
48. **Watanabe, Y., and M. Yamamoto.** 1994. *S. pombe mei2*$^+$ encodes an RNA-binding protein essential for premeiotic DNA synthesis and meiosis I, which cooperates with a novel RNA species meiRNA. Cell **78:**487–498.
49. **Wigge, P. A., and J. V. Kilmartin.** 2001. The Ndc80p complex from *Saccharomyces cerevisiae* contains conserved centromere components and has a function in chromosome segregation. J. Cell Biol. **152:**349–360.
50. **Wilusz, C. J., M. Wormington, and S. W. Peltz.** 2001. The cap-to-tail guide to mRNA turnover. Nat. Rev. Mol. Cell Biol. **2:**237–246.
51. **Wyers, F., M. Rougemaille, G. Badis, J. C. Rousselle, M. E. Dufour, J. Boulay, B. Regnault, F. Devaux, A. Namane, B. Seraphin, D. Libri, and A. Jacquier.** 2005. Cryptic pol II transcripts are degraded by a nuclear quality control pathway involving a new poly(A) polymerase. Cell **121:**725–737.